Check for updates

# Simulation of Physiological Loading in Total Hip Replacements

**A. Ramos**
Departamento de Engenharia Mecânica
Universidade de Aveiro,
3810-193 Aveiro,
Portugal

**F. Fonseca**
Faculdade de Ciências da Saúde
Universidade da Beira Interior,
6201-001 Covilhã,
Portugal

**J. A. Simões**[1]
Departamento de Engenharia Mecânica
Universidade de Aveiro,
3810-193 Aveiro,
Portugal
e-mail: simoes@mec.ua.pt

*The determination of biomechanical force systems of implanted femurs to obtain adequate strain measurements has been neglected in many published studies. Due to geometric alterations induced by surgery and those inherent to the design of the prosthesis, the loading system changes because the lever arms are modified. This paper discusses the determination of adequate loading of the implanted femur based on the intact femur-loading configuration. Four reconstructions with Lubinus SPII, Charnley Roundback, Müller Straight and Stanmore prostheses were used in the study. Pseudophysiologic and nonphysiologic implanted system forces were generated and assessed with finite element analysis. Using an equilibrium system of forces composed by the Fx (medially direction) component of the hip contact force and the bending moments Mx (median plane) and My (coronal plane) allowed adequate, pseudo-physiological loading of the implanted femur. We suggest that at least the bending moment at the coronal plane must be restored in the implanted femur-loading configuration.* [DOI: 10.1115/1.2205864]

*Keywords: physiological loading, strain, finite element analysis, femoral prosthesis, total hip replacement*

## 1 Introduction

Finite element analysis (FEA) is a powerful tool and even though the use of it has been criticized because of the lack of validation, it is the only way forward to explore "possible" solutions, even if quantitative results cannot be obtained due to the missing of biological information [1,2]. Besides other merits, finite element models can be used to distinguish and predict the performance of implants.

FE analyses depend on simulation parameters like tissue geometry replication, material properties, boundary conditions (loading and fixation), and finite element selection. Musculoskeletal tissues have irregular geometry and so finite element modeling is increasingly carried out using digitized images generated from computer tomography scanning [1]. Bone materials are normally assumed to be isotropic and homogeneous medias, whereas it is known that they are highly anisotropic and inhomogeneous, in particular cancellous bone (see, e.g., [3]). Time-dependent mechanical properties of tissues are also seen as critical to the improvement of biomechanical models [1,4]. Loading and fixation conditions are relevant input data that can strongly influence results [5,6]. Loads applied to finite element models have been strongly simplified and many papers report all sorts of loading configurations, namely, in total hip and knee replacements (see e.g., [7,8]) and seem to be a strong limitation on the quantitative accuracy of finite element results. Some researchers have focused on the development of improved geometric precision, whereas others have focused on improved representations of material behavior [1].

There are other factors intrinsically related to the FEA itself. The finite element mesh is a key factor for an efficient analysis and much research has been done on meshing and element performance (see, e.g., [9–23]). Finite element models must be sufficiently refined to accurately represent the geometry and mechanical behavior of the bone structure [17,19]. The results of these models are mesh sensitive and convergence tests must be made to test the model accuracy [16]. Convergence tests can be done comparing nodal displacements and/or total strain energy [18,19], or stresses and strains [19].

The biomechanics of the hip is an extremely complex system and the correct knowledge of the functioning of muscles, ligaments, and the hip contact force (HCF) is unknown. Many authors have studied this problem using numerical and experimental models [8,24–27]. Simulation of physiological loading of the hip is of considerable importance to improve prostheses design, bone remodeling simulations and mechanical testing of implants [27].

Other aspect of loading of the implanted femur is related to the change of forces (magnitude and direction) of the hip when a replacement is performed. The HCF and muscle forces are modified due to geometric alterations, as for example, changes of the position of the head or of the great trochanter provoked by surgery. The prosthesis does not exactly restore the original head center and lever arms are different. Although the effect of a femoral head displacement is important from a surgical point of view [28], this variable must be controlled when numerical or experimental studies are performed and since the head location cannot be restored exactly, it is necessary to analyze how it can be misleading in assessing the performance of different designs [28–30].

The intact femur undergoes a system of loads and moments that cannot be transposed in simulations of the implanted femur. We remind that the femur is statically undetermined due to the joint, ligaments, and muscle forces. There is no perfect solution when one tries to replicate the three forces and three moments as in the intact femur with identical femora implanted with different stems. Following Cristofolini and Viceconti [5], there are two main options: one that applies the same force magnitude for the hip joint and the abducting force (same forces) and a different moment will be applied due to the changed lever arms; and one that applies the same bending moment to the femur and different force values are required. In this case, the magnitude, direction, and position of the resultant vector force must stay constant with respect to the femoral diaphysis [5].

There seems to be no agreement in the literature on the preferred solution [31]. However, Cristofolini and Viceconti [5] refer that to compensate for the unavoidable geometry changes, the implanted femur should be loaded in such a way as to apply the

[1]Corresponding author.

Contributed by the Bioengineering Division of ASME for publication in the JOURNAL OF BIOMECHANICAL ENGINEERING Manuscript received May 5, 2005; final manuscript received January 2, 2006. Review conducted by Jeffrey A. Weiss.

 Copyright © 2006 by ASME 

Downloaded from http://risk.asmedigitalcollection.asme.org/biomechanical/article-pdf/128/4/579/5614399/579_1.pdf by guest on 02 November 2024

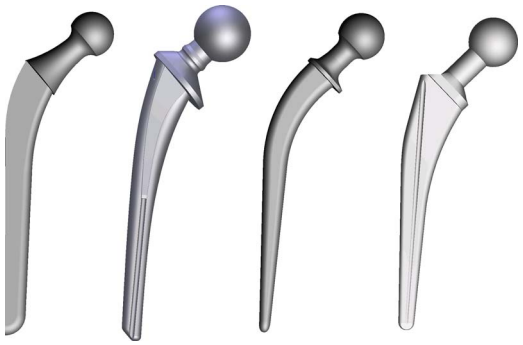

**Fig. 1 CAD models of Charnley Roundback, Lubinus SPII, Stanmore and Müller Straight cemented prostheses**

same bending moment, rather than the same forces as in the intact femur. If this is not done, errors can be expected in the strain measurement that possibly overshadow existing differences between implants, or give the impression that the difference exists when, in fact, the variations observed depend merely on the loading setup [5]. In several cases in the literature, large strain differences are found below the stem tip in the implanted femur in comparison to the intact femur [32–34].

A detailed numerical study was performed to determine how load configurations of the implanted femur can undermine the reliability of strain measurements. Based on the intact femur loading configurations of walking during gait, implanted femora with Lubinus SPII, Charnley Roundback, Müller Straight, and Stanmore loading configurations were analyzed. A set of plausible combinations of forces with bending and torsion moments was simulated and analyzed. The difference of strain in all aspects of the intact and the implanted femur was compared to select the suitable loading configuration(s) for each of the prostheses assessed in this study.

## 2 Materials and Methods

The assessment of different types of cemented hip arthroplasties was made through finite element analysis. Three-dimensional (3D) computer aided design (CAD) models representing cemented hip joint reconstructions with Charnley Roundback, Lubinus SPII, Stanmore, and Müller Straight (Fig. 1) prostheses were used. For this purpose, in vitro femoral replacements were performed on synthetic composite femurs (third generation, left, mod. 3306, Pacific Research Labs, Vashon Island, WA) by a surgeon that followed strictly the surgical protocol of each one of the prostheses. The replacements provoked offsets ranging from 28.25 mm (Charnley Roundback) to 35.48 mm (Stanmore). The large left composite femur (mod. 3306, Pacific Research Labs, Vashon Island, WA) was used as reference geometry for the finite element analysis [35]. It is a 3D solid model made available in public domain derived from computer tomography (CT)-scan dataset of the composite femur. The CAD models of the prostheses were obtained by reverse engineering. The geometry of the cement mantle and position of the stem in the femur were determined from CT scans of the reconstructions.

The numerical simulations were preformed with Hyperworks® 5.1 (Altair Engineering, Inc., Troy, MI) finite element analysis software, using pre- and post-processor HYPERMESH® 5.1 and solver HYPERSTRUCT® 5.1, respectively. Four-node linear tetrahedral elements were selected to generate the numerical models. In Table 1 the number of nodes and elements for the implanted femurs are identified. Convergence tests of the finite element meshes were previously performed and the models refinement was sufficient enough to obtain accurate stress and strain predictions. The experimental models were validated successfully by strain gauge measurements.

The cortical and cancellous bone replicating materials, femoral component and cement mantle were assumed to be isotropic and linearly elastic. The elastic properties of all materials of the reconstructions are presented in Table 2. The loading configuration used in the study represents the one around the hip during the most strenuous phase of the walking cycle (Table 3) [36]. The loading comprises the hip contact force (HCF), the glutei, the tensor fasciae latae, and the vastus lateralis (Fig. 2) and was proposed by Bergmann et al. [37,38] and Heller et al. [39] for mechanical testing of hip replacement reconstructions [36].

One possible way to determine the implanted femur loading system is to compare the strain measured below the femoral stem tip before and after implantation. Theoretically, these values must be identical because they belong to an area far from the influence of the implant [5]. To determine the changed biomechanical forces of the implanted femur, the moments and forces transmitted through the intact femur must be determined. The moments and forces, at a region of the cortex of the intact femur, far enough

**Table 3 Representation of the hip joint and muscle force magnitudes during walking**

| Vector forces (N) | *X* medially | *Y* anteriorly | *Z* proximally |
|---|---|---|---|
| Hip force contact (HCF) | −405 | −246 | −1719 |
| Abductors (glutei) | 435 | 32 | 649 |
| Tensor fasciae latae (proximal part) | 54 | 87 | 99 |
| Tensor fasciae latae (distal part) | −4 | −5,3 | −143 |
| Vastus Lateralis | −7 | 139 | −697 |

**Table 1 Nodes | elements of the FEA models**

| Model | Lubinus SPII | Charnley Roundback | Müller Straight | Stanmore |
|---|---|---|---|---|
| Cortical bone | 38002\|167051 | 38087\|166023 | 41328\|181625 | 36291\|157684 |
| Cancellous bone | 16452\|68996 | 16887\|74334 | 19145\|82413 | 19070\|80483 |
| Cement mantle | 26476\|105621 | 23281\|96612 | 26562\|109375 | 25147\|105868 |
| Prosthesis | 19024\|82821 | 12599\|53933 | 16831\|73279 | 14072\|60572 |

**Table 2 Mechanical properties of the finite element models**

| Part of model | Material type | Elastic modulus (GPa) | Poisson's ratio |
|---|---|---|---|
| Cortical bone | Glass-fiber reinforced epoxy | 14.2 | 0.28 |
| Cancellous bone | Polyurethane foam | 0.280 | 0.3 |
| Cement | Polymethylmethacrylate | 3.0 | 0.3 |
| Stem | CoCr alloy | 210 | 0.3 |



Downloaded from http://risk.asmedigitalcollection.asme.org/biomechanical/article-pdf/128/4/579/5614399/579_1.pdf by guest on 02 November 2024

from the tip of the prosthesis and from the region of the fixed condyles can be compared with those of the implanted femur. To generate tentative loading configurations for the different hip replacements, intact and implanted femur strains were compared in a region of the diaphysis of the femur out of influence of the stem. To obtain the implanted HC and abductors forces, two situations were analyzed:

- Equilibrium of forces and moments considering the implanted HC vector force (direction and magnitude) variable;
- Equilibrium of forces and moments considering the implanted HC and abductors vector forces variable, but the direction of the abductor force was kept unchanged.

The magnitudes and directions of the distal and proximal tensor fasciae latae and the vastus lateralis were kept unchanged.

Considering the equilibrium forces for the intact femur, the following equations can be setup (Figs. 2 and 3):

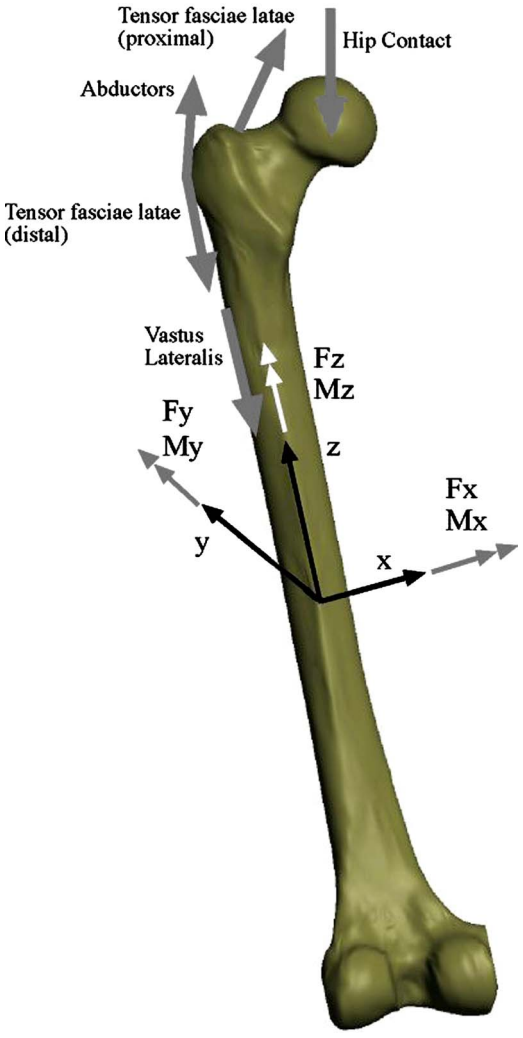


**Fig. 2 CAD model of the intact femur; moments and forces transmitted (Mz-horizontal plane; My-coronal plane, and Mx-median plane) due to loading; *x* (medially), *y* (anteriorly), and *z* (proximally)**

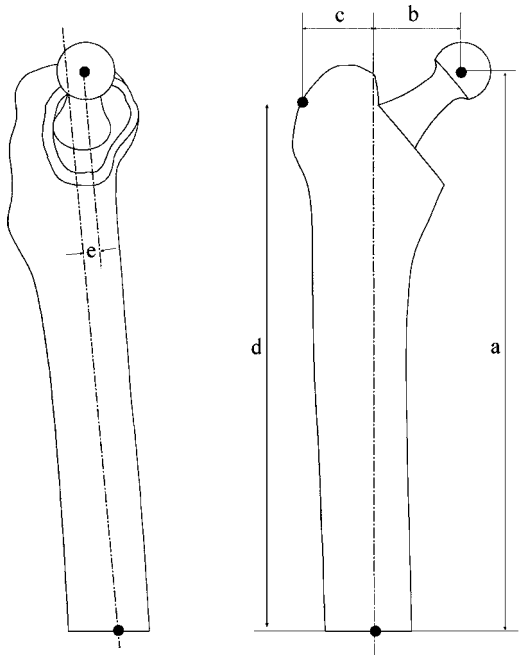


**Fig. 3 Geometric and dimensional variables of the implanted femur**

$$\begin{cases} \sum \mathrm{Fx}_{\mathrm{int\_femur}} = \mathrm{ABD}_x + \mathrm{HCF}_x \\ \sum \mathrm{Fy}_{\mathrm{int\_femur}} = \mathrm{ABD}_y + \mathrm{HCF}_y \\ \sum \mathrm{Fz}_{\mathrm{int\_femur}} = \mathrm{ABD}_z + \mathrm{HCF}_z \\ \sum \mathrm{Mx}_{\mathrm{int\_femur}} = \mathrm{HCF}_y a - \mathrm{HCF}_z e + \mathrm{ABD}_y d \\ \sum \mathrm{My}_{\mathrm{int\_femur}} = -\mathrm{HCF}_x a - \mathrm{HCF}_z b - \mathrm{ABD}_x d + \mathrm{ABD}_z c \\ \sum \mathrm{Mz}_{\mathrm{int\_femur}} = \mathrm{HCF}_y b - \mathrm{ABD}_y c \end{cases} \quad (1)$$

If the abductor force direction is considered unchanged:

$$\begin{cases} \mathrm{ABD}_y = \alpha \mathrm{ABD}_z \\ \mathrm{ABD}_x = \beta \mathrm{ABD}_z \end{cases} \quad (2)$$

where $k_1$ and $k_2$ are constants. For the abductors direction force considered, $k_1 = -1.490$ and $k_2 = -0.0741$. Figure 3 shows the geometric dimensions (Table 4) used to derive the force systems of the reconstructed femurs. Dimensions $c$ and $d$ (distances from the glutei insertion point) were kept constant. The system of Eqs. (1) allows 35 possible combinations, where 27 have solutions and 8 have indeterminate solutions. All solutions were analyzed, but only the first nine load cases (Table 5) are discussed in this paper that includes physiological and non-physiological load configuration systems.

For load Case_1, load Case_2, load Case_3, and load Case_4 the HCF was allowed to change in magnitude and direction and the other muscle forces were kept unchangeable. For the other cases studied, the HCF and the abductors force was allowed to

**Table 4 Geometric dimensions of intact and implanted femurs**

| | a | b | c | d | e |
|---|---|---|---|---|---|
| Intact femur | 230 | 44 | 25 | 205 | 0 |
| Charnley Roundback | 227.16 | 28.25 | 25 | 205 | 0.50 |
| Lubinus SPII | 223.55 | 33.37 | 25 | 205 | −1.51 |
| Stanmore | 230.48 | 35.48 | 25 | 205 | 0.61 |
| Muller Straight | 221.83 | 32.79 | 25 | 205 | −4.71 |

Downloaded from http://risk.asmedigitalcollection.asme.org/biomechanical/article-pdf/128/4/579/5614399/579_1.pdf by guest on 02 November 2024

change in magnitude, maintaining the direction of the abductors force unchangeable. Table 6 contains the HCF and abductor forces derived using Eqs. (1) and (2) for the four hip reconstructions analyzed and for the load cases selected for discussion. These load cases were simulated and strains compared with those obtained for the intact femur. Table 7 contains all the other (18) possible load configurations.

An equivalent strain value that takes into account the strain values at the medial, lateral, anterior, and posterior aspects of the femur was obtained using the following equation:

$$\Delta\varepsilon = \frac{\sqrt{(\epsilon M_{int} - \epsilon M_{imp})^2 + (\epsilon L_{int} - \epsilon L_{imp})^2 + (\epsilon A_{int} - \epsilon A_{imp})^2 + (\epsilon P_{int} - \epsilon P_{imp})^2}}{4} \quad (3)$$

being eM, eL, eA, and eP the strain at the medial, lateral, anterior, and posterior aspects of the intact (int) and implanted (imp) femur. This root-mean-squared strain value approximates in excess the difference between the intact and implanted strains.

The intact femur load system was used for the implanted configurations and is referred as load Case_0. The other load cases were simulated to illustrate the relevance of the vector components of the HCF on the bending (all load configurations) and torsional moments (Case_1, Case_2, Case_6, and Case_9). Some of the load cases were simulated to show that although the force system is in equilibrium, they can provoke nonphysiological load configurations (e.g., Case_7 for the Charnley Roundback and Stanmore prostheses and Case_8 for all designs). The strains were compared in the $x$, $y$, and $z$ directions. The most suitable loading configuration of the implanted femur will be the one that minimizes the difference in strains (intact femur strain minus implanted femur strain).

## 3 Results and Discussion

Considering the HC and abductors forces derived from Eqs. (1) and (2) and although the system forces is in equilibrium, loading configurations for which the sense of the force is opposite to the physiological one can be obtained (for Case_7 and Stanmore prosthesis we can observe that the sense of the HCF is toward proximal, whereas physiologically it is toward distal) and the intensity is significantly different than what is observed in vivo (e.g., Case_2, Case_6, and Case_9 provoke very high intensity forces and Case_7 and Case_8 provoke very low intensity forces). Other load cases show considerable high or low force magnitudes that are unlikely to occur in vivo. Interesting to note that independently on the prosthesis design, the $z$ component of the HCF is considerable higher for all implanted configurations. The $z$ component of the HCF of the implanted reconstruction for load Case_4, relatively to the intact femur, is higher in an excess of 918, 469, 418, and 487 N for the Lubinus SPII, Charnley Roundback, Müller Straight, and Stanmore prostheses, respectively.

**Table 5 Moments and forces considered in the tentative load cases studied**

| | Fx | Fy | Fz | Mx | My | Mz |
|---|---|---|---|---|---|---|
| Case_0 | Intact hip force system | | | | | |
| Case_1[a] | | | X | | X | X |
| Case_2[a] | X | | | | X | X |
| Case_3[a] | | | X | X | X | |
| Case_4[a] | X | | | X | X | |
| Case_5 | X | X | X | | X | |
| Case_6 | | | X | X | X | X |
| Case_7 | X | | X | X | X | |
| Case_8 | | X | X | X | X | |
| Case_9 | X | | X | X | | X |
| Case_10 | X | X | X | | | |
| Case_11 | X | X | | X | | |
| Case_12 | X | X | | | X | |
| Case_13 | X | | X | X | | |
| Case_14 | X | | X | X | | |
| Case_15 | | X | X | X | | |
| Case_16 | X | | | X | | X |
| Case_17 | | X | | X | X | |
| Case_18 | | | | X | X | X |
| Case_19 | X | X | X | X | | |
| Case_20 | X | X | X | | | X |
| Case_21 | X | X | | X | X | |
| Case_22 | X | X | | X | | X |
| Case_23 | X | X | | | X | X |
| Case_24 | X | | X | X | X | |
| Case_25 | | X | X | | X | X |
| Case_26 | X | | | X | X | X |
| Case_27 | | X | | X | X | X |

[a]Abductors force magnitude and direction unchanged.

For the load cases presented in Table 6, the strain values in the $x$, $y$, and $z$ directions were picked at a distance of 20 mm down from the tip of the longest stem (Lubinus SPII). This region of the femur is out of the influence of the stem, which was confirmed numerically with finite element models and with uniaxial strain gauges glued to composite replica femurs. The absolute difference ($De_z = |e_{z\ intact} - e_{z\ implanted}|$) between strains generated by the intact and implanted femurs are presented in Table 8. Table 9 presents the mean-squared strain difference for the tentative solutions analyzed.

Ideally, the most adequate implanted femur-loading configuration should provoke the same strain magnitudes as the ones provoked by the intact femur. However, this is not possible, unless extra forces are added to the loading system. Therefore, the suitable loading configuration is the one that minimizes the differences in strains in all aspects of the femur. Due to the higher magnitudes of strains in the axial direction of the femur ($z$ direction) at the lateral and medial aspects of the femur, the $\varepsilon_z$ component of the strain seems to be an adequate parameter to select the suitable loading configuration for each of the hip replacements assessed.

Figure 4($a$) shows the strain ($\varepsilon_z$) distribution at the medial aspect of the femur considering all the reconstructions loaded with the loading configuration of the intact femur (Case_0), which does not take into account the correction of the load system. Figure 4($b$) illustrates identical results but with the loading configuration corrected (Case_4). The comparison of these two figures show that it can be misleading in assessing the performance of different designs if the implanted loading system is not derived adequately. Figure 4($b$) also shows the strain shielding effect, which does not depend on the stem geometry since very similar strain magnitudes were observed for all designs.

For the hip replacements simulated with loading configuration of the intact femur simulated, the Lubinus SPII provoked the highest strain differences in all aspects of the femur; the Charnley Roundback and Müller Straight provoked very similar differences and the Stanmore provoked differences of strains higher at the proximal portion of the femur. The results presented in Fig. 4



Downloaded from http://risk.asmedigitalcollection.asme.org/biomechanical/article-pdf/128/4/579/5614399/579_1.pdf by guest on 02 November 2024

**Table 6 HC and abductors force components used in the simulations of reconstructed femurs (first nine load cases of Table 5)**

| | | Lubinus SPII | | Charnley Roundback | | | Müller Straight | | | Stanmore | | | |
|---|---|---|---|---|---|---|---|---|---|---|---|---|---|
| Force (N) | | Med. | Ant. | Prox. | Med. | Ant. | Prox. | Med. | Ant. | Prox. | Med. | Ant. | Prox. |
| Case_0 | HFC | −405 | −246 | −1719 | −405 | −246 | −1719 | −405 | −246 | −1719 | −405 | −246 | −1719 |
| | ABD | 435 | 32 | 649 | 435 | 32 | 649 | 435 | 32 | 649 | 435 | 32 | 649 |
| Case_1 | HFC | −291 | −383 | −1719 | 137 | −349 | −1719 | 117 | −328 | −1719 | 142 | −355 | −1719 |
| | ABD | 435 | 32 | 649 | 435 | 32 | 649 | 435 | 32 | 649 | 435 | 32 | 649 |
| Case_2 | HFC | −405 | −383 | −2637 | −405 | −349 | −5347 | −405 | −328 | −5108 | −405 | −355 | −5420 |
| | ABD | 435 | 32 | 649 | 435 | 32 | 649 | 435 | 32 | 649 | 435 | 32 | 649 |
| Case_3 | HFC | −291 | −253 | −1719 | −335 | −265 | −1719 | −341 | −250 | −1719 | −333 | −292 | −1719 |
| | ABD | 435 | 32 | 649 | 435 | 32 | 649 | 435 | 32 | 649 | 435 | 32 | 649 |
| Case_4 | HFC | −405 | −255 | −2637 | −405 | −268 | −2188 | −405 | −251 | −2137 | −405 | −302 | −2206 |
| | ABD | 435 | 32 | 649 | 435 | 32 | 649 | 435 | 32 | 649 | 435 | 32 | 649 |
| Case_5 | HFC | −858 | −280 | −2394 | −634 | −263 | −2060 | −634 | −263 | −2061 | −635 | −263 | −2062 |
| | ABD | 888 | 66 | 1324 | 664 | 49 | 990 | 664 | 49 | 991 | 665 | 49 | 992 |
| Case_6 | HFC | −1492 | −320 | −3150 | −1289 | 284 | −2808 | −918 | −282 | −2391 | −1901 | −263 | −3500 |
| | ABD | 1394 | 103 | 2080 | 1166 | 87 | 1738 | 886 | 66 | 1321 | 1630 | 121 | 2430 |
| Case_7 | HFC | −1461 | −324 | −2071 | 2851 | −4 | −4016 | −972 | −288 | −1949 | −5362 | −614 | 887 |
| | ABD | 1491 | 111 | 2223 | −2821 | −209 | −4207 | 1002 | 74 | 1494 | 5392 | 400 | 8042 |
| Case_8 | HFC | −2465 | −375 | −4309 | 29 | −225 | −1304 | −1558 | −316 | −3136 | 633 | −192 | −622 |
| | ABD | 2172 | 161 | 3239 | 157 | 12 | 234 | 1385 | 103 | 2066 | −301 | −22 | −449 |
| Case_9 | HFC | −1365 | −320 | −3150 | −1136 | −284 | −2808 | −856 | −282 | −2391 | −1600 | −263 | −3500 |
| | ABD | 1394 | 103 | 2080 | 1166 | 87 | 1738 | 886 | 66 | 1321 | 1630 | 121 | 2430 |

**Table 7 The other HC and abductors force components of reconstructed femurs**

| | | Lubinus SPII | | Charnley Roundback | | | Müller Straight | | | Stanmore | | | |
|---|---|---|---|---|---|---|---|---|---|---|---|---|---|
| Force (N) | | Med. | Ant. | Prox. | Med. | Ant. | Prox. | Med. | Ant. | Prox. | Med. | Ant. | Prox. |
| Case_10 | HFC | −405 | 246 | 1719 | −405 | 246 | 1719 | −405 | 246 | 1719 | −405 | 246 | 1719 |
| | ABD | 435 | −32 | −649 | 435 | −32 | −649 | 435 | −32 | −649 | 435 | −32 | −649 |
| Case_11 | HFC | −405 | 246 | −1397 | −405 | 246 | 1051 | −405 | 246 | 194 | −405 | 246 | 427 |
| | ABD | 435 | −32 | −649 | 435 | −32 | −649 | 435 | −32 | −649 | 435 | −32 | −649 |
| Case_12 | HFC | −405 | 246 | 148972 | −405 | 246 | −48360 | −405 | 246 | 124312 | −405 | 246 | −15356 |
| | ABD | 435 | −32 | −649 | 435 | −32 | −649 | 435 | −32 | −649 | 435 | −32 | −649 |
| Case_13 | HFC | −405 | 253 | 1719 | −405 | 241 | 1719 | −405 | 250 | 1719 | −405 | 219 | 1719 |
| | ABD | 435 | −32 | −649 | 435 | −32 | −649 | 435 | −32 | −649 | 435 | −32 | −649 |
| Case_14 | HFC | −405 | 383 | 1719 | −405 | 324 | 1719 | −405 | 305 | 1719 | −405 | 330 | 1719 |
| | ABD | 435 | −32 | −649 | 435 | −32 | −649 | 435 | −32 | −649 | 435 | −32 | −649 |
| Case_15 | HFC | −81 | 246 | 1719 | −67 | 246 | 1719 | −81 | 246 | 1719 | −42 | 246 | 1719 |
| | ABD | 435 | −32 | −649 | 435 | −32 | −649 | 435 | −32 | −649 | 435 | −32 | −649 |
| Case_16 | HFC | −405 | 383 | 60913 | −405 | 324 | −10551 | −405 | 305 | 22514 | −405 | 330 | −3534 |
| | ABD | 435 | −32 | −649 | 435 | −32 | −649 | 435 | −32 | −649 | 435 | −32 | −649 |
| Case_17 | HFC | −74 | 246 | −1397 | −71 | 246 | 1051 | −77 | 246 | 194 | −70 | 246 | 427 |
| | ABD | 435 | −32 | −649 | 435 | −32 | −649 | 435 | −32 | −649 | 435 | −32 | −649 |
| Case_18 | HFC | −211 | 383 | 60913 | −150 | 324 | −10551 | −136 | 305 | 22514 | −154 | 330 | −3534 |
| | ABD | 435 | −32 | −649 | 435 | −32 | −649 | 435 | −32 | −649 | 435 | −32 | −649 |
| Case_19 | HFC | −2142 | 375 | 4309 | −127 | 225 | 1304 | −1355 | 316 | 3136 | 331 | 191 | 622 |
| | ABD | 2172 | −161 | −3239 | 157 | −12 | −234 | 1385 | −103 | −2066 | −301 | 22 | 449 |
| Case_20 | HFC | −1386 | 319 | 3183 | −1009 | 291 | 2620 | −872 | 281 | 2416 | −1049 | 294 | 2679 |
| | ABD | 1416 | −105 | −2112 | 1039 | −77 | −1550 | 902 | −67 | −1346 | 1079 | −80 | −1609 |
| Case_21 | HFC | −4889 | 578 | 13336 | −4115 | 521 | −2328 | −5934 | 656 | 17316 | −3830 | 500 | −481 |
| | ABD | 4919 | −365 | −7336 | 4145 | −307 | −6182 | 5964 | −442 | −8895 | 3860 | −286 | −5757 |
| Case_22 | HFC | −1386 | 319 | 1827 | −1009 | 291 | 500 | −872 | 281 | 1641 | −1049 | 294 | 256 |
| | ABD | 1416 | −105 | −2112 | 1039 | −77 | −1550 | 902 | −67 | −1346 | 1079 | −80 | −1609 |
| Case_23 | HFC | −1386 | 319 | 119285 | −1009 | 291 | −40863 | −872 | 281 | 115266 | −1049 | 294 | −12561 |
| | ABD | 1416 | −105 | −2112 | 1039 | −77 | −1550 | 902 | −67 | −1346 | 1079 | −80 | −1609 |
| Case_24 | HFC | −5044 | 578 | 8638 | −4993 | 507 | 8561 | −6287 | 661 | 10491 | −6393 | 439 | 10650 |
| | ABD | 5074 | −376 | −7568 | 5023 | −372 | −7491 | 6317 | −468 | −9421 | 6423 | −476 | −9580 |
| Case_25 | HFC | −1131 | 322 | 3183 | −716 | 276 | 2620 | −574 | 283 | 2416 | −725 | 242 | 2679 |
| | ABD | 1416 | −105 | −2112 | 1039 | −77 | −1550 | 902 | −67 | −1346 | 1079 | −80 | −1609 |
| Case_26 | HFC | 2535 | 576 | 237895 | 6024 | 681 | −128126 | 3618 | 515 | 202172 | 7241 | 762 | −48559 |
| | ABD | −2505 | 186 | 3735 | −5994 | 444 | 8939 | −3588 | 266 | 5352 | −7211 | 535 | 10754 |
| Case_27 | HFC | −1128 | 319 | 1827 | −730 | 291 | 500 | −572 | 281 | 1641 | −111 | 294 | 256 |
| | ABD | 1416 | −105 | −2112 | 1039 | −77 | −1550 | 902 | −67 | −1346 | 1079 | −80 | −1609 |

Downloaded from http://risk.asmedigitalcollection.asme.org/biomechanical/article-pdf/128/4/579/5614399/579_1.pdf by guest on 02 November 2024

**Table 8 Absolute difference between strains generated by the intact and implanted femurs (all tentative load configurations)**

| Strain ($\mu\varepsilon$) | | Lubinus SPII | | | | Chamley | | | | Müller Straight | | | | Stanmore | | | |
|---|---|---|---|---|---|---|---|---|---|---|---|---|---|---|---|---|---|
| | | Med | Post | Ant | Lat | Med | Post | Ant | Lat | Med | Post | Ant | Lat | Med | Post | Ant | Lat |
| Case_0 | εx | 161 | 62 | 52 | 116 | 92 | 37 | 39 | 75 | 102 | 44 | 23 | 49 | 129 | 6 | 1 | 70 |
| | εy | 153 | 6 | 45 | 126 | 89 | 44 | 28 | 77 | 82 | 44 | 22 | 54 | 109 | 2 | 3 | 82 |
| | εz | 524 | 210 | 168 | 389 | 301 | 138 | 107 | 242 | 315 | 149 | 98 | 180 | 405 | 19 | 4 | 247 |
| Case_1 | εx | 65 | 115 | 115 | 24 | 444 | 85 | 123 | 455 | 427 | 1111 | 142 | 667 | 387 | 115 | 176 | 481 |
| | εy | 45 | 115 | 105 | 27 | 469 | 68 | 108 | 455 | 483 | 47 | 98 | 490 | 443 | 120 | 151 | 451 |
| | εz | 192 | 378 | 359 | 92 | 1528 | 263 | 381 | 1551 | 1498 | 185 | 342 | 1641 | 1374 | 393 | 164 | 1573 |
| Case_2 | εx | 24 | 180 | 122 | 29 | 633 | 406 | 207 | 423 | 600 | 314 | 196 | 503 | 538 | 524 | 332 | 445 |
| | εy | 1 | 176 | 115 | 34 | 681 | 378 | 200 | 438 | 683 | 300 | 158 | 503 | 626 | 518 | 309 | 423 |
| | εz | 51 | 585 | 1513 | 90 | 2180 | 1317 | 1812 | 3717 | 2105 | 1037 | 531 | 1655 | 1905 | 1686 | 1060 | 1455 |
| Case_3 | εx | 45 | 56 | 30 | 1 | 22 | 44 | 37 | 2 | 36 | 41 | 10 | 20 | 54 | 42 | 279 | 10 |
| | εy | 30 | 52 | 32 | 8 | 18 | 51 | 29 | 5 | 12 | 41 | 14 | 14 | 33 | 38 | 19 | 5 |
| | εz | 127 | 184 | 115 | 9 | 64 | 162 | 106 | 2 | 89 | 134 | 66 | 49 | 149 | 139 | 73 | 19 |
| Case_4 | ϵx | 3 | 12 | 20 | 4 | 3 | 6 | 29 | 6 | 14 | 7 | 1 | 20 | 32 | 1 | 11 | 8 |
| | εy | 15 | 11 | 19 | 14 | 9 | 15 | 20 | 7 | 13 | 8 | 6 | 15 | 8 | 2 | 9 | 7 |
| | εz | 14 | 4 | 75 | 8 | 20 | 39 | 77 | 7 | 14 | 24 | 38 | 51 | 74 | 5 | 38 | 10 |
| Case_5 | εx | 32 | 75 | 45 | 14 | 17 | 38 | 33 | 3 | 27 | 48 | 15 | 29 | 54 | 1 | 16 | 11 |
| | εy | 16 | 70 | 47 | 8 | 10 | 46 | 25 | 4 | 2 | 48 | 21 | 25 | 26 | 4 | 14 | 1 |
| | εz | 84 | 245 | 167 | 58 | 44 | 146 | 93 | 23 | 59 | 159 | 87 | 82 | 144 | 2 | 44 | 23 |
| Case_6 | εx | 20 | 81 | 50 | 28 | 2 | 60 | 52 | 23 | 21 | 48 | 14 | 37 | 21 | 55 | 29 | 45 |
| | εy | 2 | 77 | 52 | 24 | 8 | 69 | 44 | 29 | 7 | 47 | 20 | 36 | 17 | 50 | 35 | 57 |
| | εz | 40 | 267 | 185 | 107 | 8 | 223 | 159 | 96 | 34 | 157 | 84 | 110 | 25 | 187 | 118 | 163 |
| Case_7 | εx | 72 | 174 | 65 | 36 | | | | | 48 | 99 | 27 | 41 | | | | |
| | εy | 60 | 163 | 71 | 35 | | | | | 24 | 97 | 34 | 39 | | | | |
| | εz | 218 | 564 | 245 | 139 | | | | | 129 | 325 | 130 | 124 | | | | |
| Case_8 | εx | 0 | 101 | 66 | 48 | 38 | 27 | 29 | 27 | 3 | 56 | 19 | 55 | | | | |
| | εy | 20 | 95 | 68 | 48 | 36 | 35 | 20 | 33 | 28 | 53 | 26 | 60 | | | | |
| | εz | 29 | 333 | 241 | 183 | 120 | 106 | 77 | 93 | 26 | 182 | 104 | 177 | | | | |
| Case_9 | εx | 112 | 85 | 33 | 160 | 151 | 63 | 37 | 181 | 45 | 49 | 5 | 105 | 274 | 64 | 4 | 360 |
| | εy | 136 | 79 | 44 | 158 | 165 | 73 | 36 | 185 | 75.5 | 49 | 17 | 101 | 326 | 56 | 14 | 359 |
| | εz | 408 | 271 | 154 | 556 | 529 | 232 | 122 | 626 | 187 | 161 | 68 | 334 | 986 | 405 | 42 | 1204 |

clearly show that it is not correct to use the same loading configuration for the intact and implanted femurs. Apparently, and observing Fig. 4(*a*) we are forced to conclude that the Lubinus SPII prosthesis provokes higher strain shielding, when in fact this does not really occur. Figure 4(*b*) shows that strain shielding is very similar for all prostheses if the loading configuration is corrected. Since the head location of the prosthesis cannot be restored, the lever arms change and also the force system and if this difference is not considered, errors can be expected in the strain measurements as evidenced in Fig. 4(*a*). It is necessary to determine how the consequences of this unavoidable source of error can be minimized [5]. Many authors have realized numerical and experimental studies using the same force system for the intact and implanted femurs [40–48].

Load Case_4, that considers the force Fx and moments Mx and My (with the abductor force direction kept unchanged), was of all loading configurations simulated the one that provoked the lowest strain deviations either using the absolute strain difference (Table 7) or the root-mean-squared strain (Table 8) parameter. Other loading configurations, like load Case_1 and load Case_2, provoked significant differences in strains and seem to be nonsuitable implantable load configurations. It is interesting to note that the load cases that provoke the lowest strain differences all include the bending moment My, reinforcing that this bending moment at the coronal plane must be restored in simulations of implanted hip reconstructions. This moment plays a key role because it is obtained using the highest vector force magnitudes and lever arms.

**Table 9 Root-mean-squared strain difference (all tentative load configurations)**

| Load Case | Lubinus SPII | Charnley Round. | Müller Straight | Stanmore |
|---|---|---|---|---|
| Case_0 | 279 | 171 | 189 | 159 |
| Case_1 | 226 | 886 | 981 | 993 |
| Case_2 | 499 | 1630 | 1254 | 1174 |
| Case_3 | 99 | 82 | 123 | 71 |
| Case_4 | 31 | 36 | 33 | 28 |
| Case_5 | 123 | 71 | 60 | 82 |
| Case_6 | 135 | 115 | 110 | 85 |
| Case_7 | 265 | 1001 | 1411 | 156 |
| Case_8 | 177 | 81 | 1221 | 111 |
| Case_9 | 300 | 342 | 637 | 170 |

Cristofolini and Viceconti [5] suggest that to compensate for the unavoidable geometry changes, the implanted femur should be loaded in such a way as to apply the same bending moment as in the intact femur. In fact, the strain deviations for load cases that included the two bending moments (Case_3, Case_4, Case_6, Case_7, and Case_8) were significantly lower. Load Case_5 that includes all forces (Fx, Fy, and Fz) and the My moment allowed relatively lower strain deviations, partially due to the influence of this bending moment (My). Overall, the load cases considering the torsional moment (Mz) (Case_1, Case_2, and Case_9) provoked very high strain deviations and it is therefore questionable the relevance of replicating this moment in the implanted femur system force, although it plays an important key role in the fixation of prostheses. It must be said that the load transfer mechanism between the intact and implanted femur is inherently different and the bending moments are reflected more pronouncedly in the strain pattern, while the torsional moment is more deleterious at the bone-prosthesis interface.

Figure 5 shows the highest strain error committed if the load system of the intact femur is used in implanted femur simulations.

Downloaded from http://risk.asmedigitalcollection.asme.org/biomechanical/article-pdf/128/4/579/5614399/579_1.pdf by guest on 02 November 2024

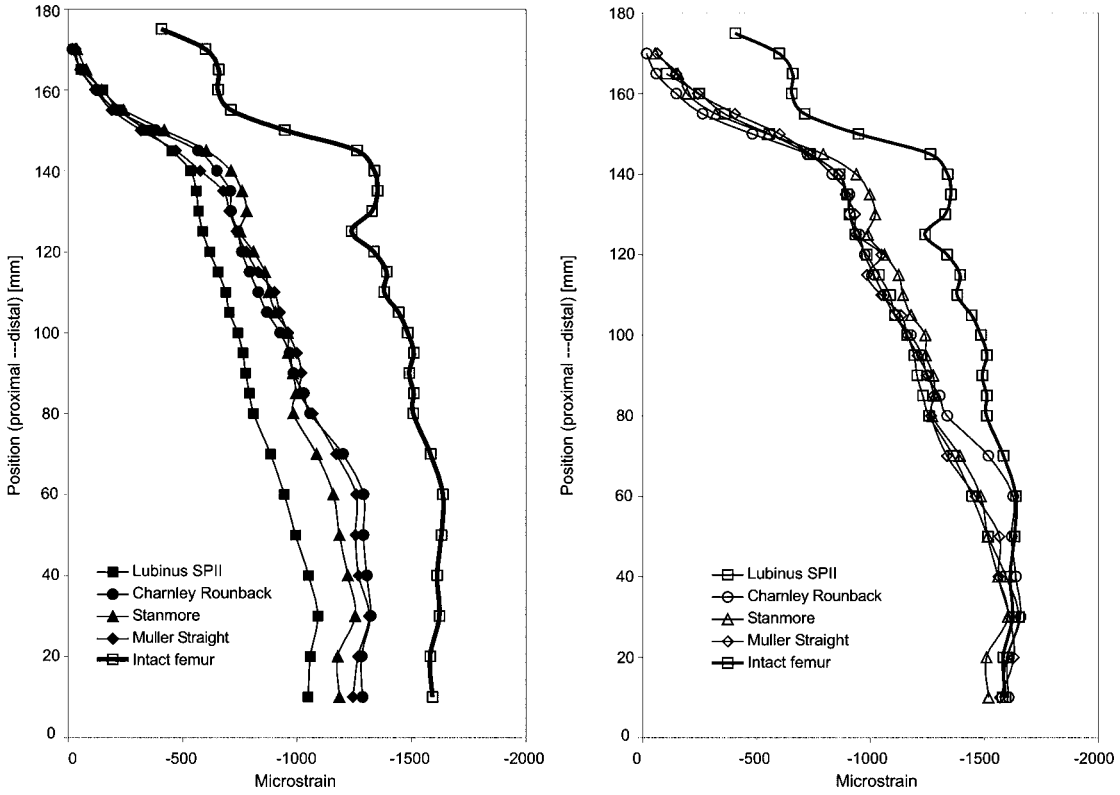


**Fig. 4 Strain distribution at the medial aspect of the implanted femur: (*a*) intact femur load system; (*b*) implanted femur load (Case_4) system**

Depending on the type of geometry, some designs provoke higher errors than others. The highest errors were observed at the medial aspect of the femur and for the Lubinus SPII stem. Errors were smaller at the anterior and posterior aspects of the femur. We can also observe that the Lubinus SP II stem provoked the highest error differences which seem too be related to its anatomical geometry. All other stems provoked similar strain differences.

The study showed that it is important to derive correctly the implanted femur-loading configuration, especially if different designs are being compared. For a certain design, including bending in the coronal plane can be sufficient; for others probably not. It is necessary to understand which the most critical load component is and try to restore the constant conditions for that one, having in mind that for others the deviations are less relevant. The adequate determination of the load configuration for implanted femurs has not been realized in many studies published [40–48].

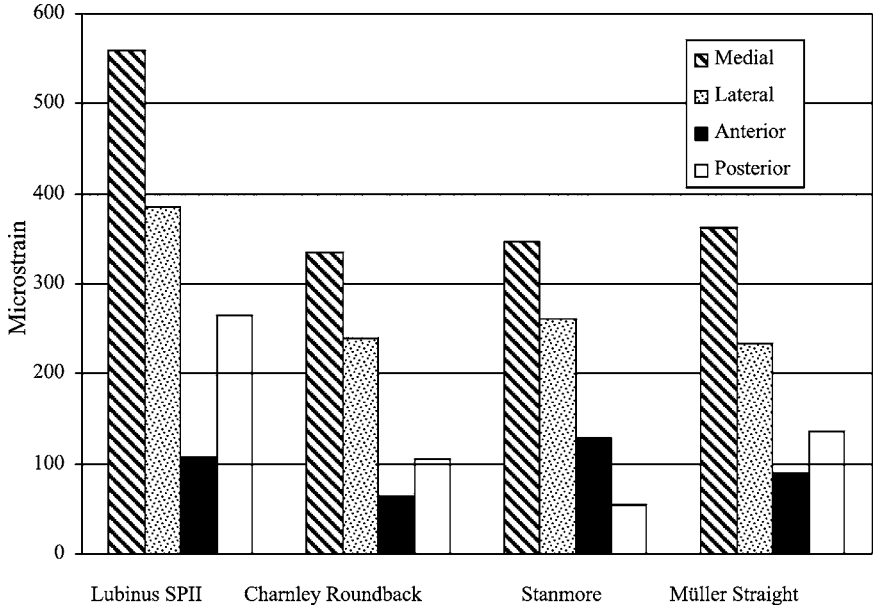


**Fig. 5 Maximum strain error measurement (intact femur strain minus implanted femur strain for load Case_4)**

Downloaded from http://risk.asmedigitalcollection.asme.org/biomechanical/article-pdf/128/4/579/5614399/579_1.pdf by guest on 02 November 2024

## 4 Concluding Remarks

The study performed aimed to derive adequate loading configurations for implanted femurs with different hip femoral components. If so is not done, errors can be expected in the strain distributions that possibly hide differences between different femoral designs. For the designs analyzed, adequate implanted system forces were generated using for the equilibrium system the Fx (medially direction) of the HCF and the bending moments (Mx and My) provoked by the HCF and abductors forces. We suggest that at least the bending moment at the coronal plane must be restored in the implanted femur-loading configuration.


## Acknowledgment

The authors gratefully acknowledge Fundação para a Ciência e a Tecnologia do Ministério da Ciência e do Ensino Superior for funding António Ramos with Grant No. SFRH/BD/63217/2002. Part of the work was supported by Project No. POCTI/EME/38367/2001 and No. POCTI/EME/44644/2002.


## References


[1] Prendergast, P. J., 1997, "Finite Element Models in Tissue Mechanics and Orthopaedic Implant Design," Clin. Biomech. (Bristol, Avon), **12**(6), pp. 343–366.

[2] Huikes, R., 1995, "The Law of Adaptive Bone Remodelling: A Case for Crying Newton? *Bone Structure and Remodelling*, A. Odgaaard, and H. Weinans, eds., World Scientific, Singapore, p. 15.

[3] van Rietbergen, B., Odgaard, A., Kabel, J., and Huiskes, R., 1996, "Direct Mechanics Assessment of Elastic Symmetries and Properties of Trabecular Bone," J. Biomech., **29**, pp. 1653–1657.

[4] Fung, Y. C., 1983, "On the Foundations of Biomechanics," J. Appl. Phys., **50**, pp. 1003–1009.

[5] Cristofolini, L., and Viceconti, M., 1999, "In-Vitro Stress Shielding Measurements Can be Affected by Large Errors," J. Arthroplasty, **14**(2), pp. 215–219.

[6] Ramos, A., and Simões, J. A., 2003, "HYPERMESH® Finite Element Model of the Proximal Femur: Some Considerations," presented at the *International Congress on Computational Bioengineering*, Zaragoza, Spain, September 24–26.

[7] Berelmans, W. A. M., Poort, H. W., and Slooff, T. J., 1972, "A New Method to Analyse the Mechanical Behaviour of Skeletal Parts," Acta Orthop. Scand., **43**, pp. 301–317.

[8] Taylor, M., Tanner, K. E., Freeman, M. A., and Yettram, A. L., 1995, "Stress and Strain Distribution Within the Intact Femur: Compression or Bending?," Med. Eng. Phys., **18**, pp. 122–131.

[9] Polgar, K., Viceconti, M., and O'Connor, J. J., 2001, "A Comparison Between Automatically Generated Linear and Parabolic Tetrahedral When Used to Mesh a Human Femur," Proc. Inst. Mech. Eng., Part H: J. Eng. Med., **215H**, pp. 85–94.

[10] Prendergast, P. J., and Maher, S. A., 2001, "Issues in Pre-Clinical Testing of Implants," J. Mater. Process. Technol., **118**, pp. 337–342.

[11] Viceconti, M., Bellingeri, L., Cristofolini, L., and Toni, A., 1998, "A Comparative Study on Different Methods of Automatic Mesh Generation of Human Femurs," Med. Eng. Phys., **20**, pp. 1–10.

[12] Merz, B., Lengsfeld, M., Müller, M. R., Kaminsky, J., Rüegsegger, P., and Niederer, P., 1996, "Automated Generation of 3D Fe-Models of the Human Femur—Comparison of Methods and Results," *Computer Methods in Biomechanics and Biomedical Engineering*, J. Middleton, M. L. Jones, and G. N. Pande, eds., Gordon and Breach Science Publishers, Amsterdam, p. 125.

[13] Keyak, J. H., and Skinner, H. B., 1992, "Three-Dimensional Finite Element Modelling of Bone: Effects of Element Size," J. Biomed. Eng., **14**, pp. 483–489.

[14] Ladd, A. I. C., and Kinney, J. H., 1998, "Numerical Errors and Uncertainties in Finite-Element Modelling of Trabecular Bone," J. Biomech., **31**, pp. 941–945.

[15] Vander Sloten, J., and Van Der Perre, G., 1993, "The Influence of Geometrical Distortions of Three-Dimensional Finite Elements, Used to Model Proximal Femoral Bone," Proc. Inst. Mech. Eng., Part H: J. Eng. Med., **209**, pp. 31–36.

[16] Stolk, J., Verdonschot, N., and Huiskes, R., 2001, "Management of Stress Fields Around Singular Points in a Finite Element Analysis," J. Middleton, M. L. Jones, N. G. Shrive, and G. N. Pande, eds., *Computer Methods in Biomechanics and Biomedical Engineering*, Gordon and Breach Science Publishers, London, p. 57.

[17] Huiskes, R., and Chao, E. Y. S., 1983, "A Survey of Finite Element Analysis in Orthopaedic Biomechanics: The First Decade," J. Biomech., **16**, pp. 385–409.

[18] Hart, R. T., Hennebel, V., Thongpreda, N., Van Buskirk, W. C., and Anderson, R. C., 1992, "Modeling the Biomechanics of the Mandible: A Three-Dimensional Finite Element Study," J. Biomech., **25**, pp. 261–286.

[19] Marks, L. W., and Gardner, T. N., 1993, "The Use of Strain Energy as a Convergence Criterion in the Finite Element Modelling of Bone and the Effect of Model Geometry on Stress Convergence," J. Biomed. Eng., **15**, pp. 474–476.

[20] Stolk, J., Verdonschot, N., and Huiskes, R., 1998, "Sensitivity of Failure Criteria of Cemented Total Hip Replacements to Finite Element Mesh Density," presented at the *11th Conf. of the European Society of Biomechanics*, Toulouse, France, July 8–11.

[21] Jeffers, J. R. T., and Taylor, M., 2003, "Mesh Considerations for Adaptive Finite Element Analyses of Cement Failure in Total Hip Replacement," presented at the *2003 Summer Bioengineering Conference*, Florida, June 25–29.

[22] Muccini, R., Baleani, M., and Viceconti, M., 2000, "Selection of the Best Element Type in the Finite Element Analysis of Hip Prostheses," J. Med. Eng. Technol., **24**(4), pp. 145–148.

[23] Viceconti, M., Zannoni, C., Testi, D., and Cappello, A., 1990, "A New Method for the Automatic Mesh Generation of Bone Segments From CT Data," J. Med. Eng. Technol., **23**(2), pp. 77–81.

[24] Bergmann, G., Graichen, F., and Rohlmann, A., 1993, "Hip Joint Loading During Walking and Running Measured in Two Patients," J. Biomech., **26**, pp. 969–990.

[25] Colgan, D., Trench, P., Slemon, D., McTague, D., Finlay, J. B., O'Donell, P., and Little, E. G., 1994, "A Review of Joint and Muscle Simulation Relevant to In-Vitro Stress Analysis of the Hip," Strain, **30**(2), pp. 47–61.

[26] Cristofolini, L., Viceconti, M., Toni, M., and Giunti, A., 1995, "Influence of Thigh Muscles on the Axial Strains in a Proximal Femur During Early Stance in Gait," J. Biomech., **28**(5), pp. 617–624.

[27] Simões, J. A., Vaz, M. A., Blatcher, S., and Taylor, M., 2000, "Influence of Head Constraint and Muscle Forces on the Strain Distribution Within the Intact Femur," Med. Eng. Phys., **22**, pp. 453–459.

[28] Huiskes, R., 1990, "The Various Stress Patterns of Press-Fit, Ingrown and Cemented Femoral Stems," Clin. Orthop. Relat. Res., **261**, pp. 27–38.

[29] Prendergast, P. J., and Taylor, D., 1990, "Stress Analysis of the Proximo-Medial Femur After Total Hip Replacement," J. Biomed. Eng., **12**, pp. 379–382.

[30] Tensi, H. M., Gese, H., and Aschrel, R., 1989, "Non-Linear Three Dimensional Finite Element Analysis of a Cementless Hip Prosthesis," Proc. Inst. Mech. Eng., Part H: J. Eng. Med., **203H**, pp. 215–222.

[31] Cristofolini, L., 1997, "A Critical Analysis of Stress Shielding Evaluation of Hip Prostheses," Crit. Rev. Biomed. Eng., **25**(4&5), pp. 409–483.

[32] Boggan, R. S., 1999, "An In Vitro Comparison of Surface Strain Patterns in Cementless Femoral Arthroplasty," Semin Arthroplasty, **4**, pp. 143–153.

[33] Oh, I., and Harris, W. H., 1978, "Proximal Strain Distribution in the Loaded Femur: An In Vitro Comparison of the Distribution in the Intact Femur and After Insertion of Different Hip-Replacement Femoral Components," J. Bone Jt. Surg., Am. Vol., Vol. **60**, pp. 75–85.

[34] Otani, T., Leo, A., and Whiteside, L. A., 1992, "Failure of Cementless Fixation of the Femoral Component in Total Hip Arthroplasty," Clin. Orthop. Relat. Res., **23**(2), pp. 335–346.

[35] Cheung, G., Zalzal, P., Bhandari, M., Spelt, J. K., and Papini, M., 2004, "Finite Element Analysis of a Femoral Retrograde Intramedullary Nail Subject to Gait Loading," Med. Eng. Phys., **26**, pp. 93–108.

[36] Stolk, J., Verdonschot, N., and Huiskes, R., 2002, "Stair Climbing is More Detrimental to the Cement in Hip Replacement Than Walking," Clin. Orthop. Relat. Res., **405**, pp. 294–305.

[37] Bergmann, G., Heller, M., and Duda, G. M., 2001, Preclinical Testing of Cemented Hip Replacement Implants: Pre-Normative Research for a European Standard," G. Bergamann, ed, *Final Report of Workpackage 5: Development of the Loading Configuration*, HIP98, Free University, Berlin.

[38] Bergmann, G., Deuretzbacher, G., Heller, M., Graichen, F., Rohlmann, A., Strauss, J., and Duda, G. N., 2001, "Hip Contact Forces and Gait Patterns From Routine Activities," J. Biomech., **34**, pp. 859–871.

[39] Heller, M. O., Bergmann, G., Deuretzbacher, G., Durselen, L., Pohl, M., Claes, L., Haas, N. P., and Duda, G. N., 2001, "Musculo-Skeletal Loading Conditions at the Hip During Walking and Stair Climbing," J. Biomech., **34**, pp. 883–893.

[40] Simões, J. A., and Vaz, M. A., 2002, "The Influence on Strain Shielding of Material Stiffness of Press-Fit Femoral Components," Proc. Inst. Mech. Eng., Part H: J. Eng. Med., **216**, pp. 341–346.

[41] Pérez, M. A., Grasa, J., Carcía-Aznar, J. M., Bea, J. A., and Doblaré, M., 2006, "Probabilistic Analysis of the Influence of the Bonding Degree of the Stem-Cement Interface in the Performance of Cemented Hip Prostheses," J. Biomech. (in press).

[42] Maher, A., and Prendergast, P. J., 2005, "Discriminating the Loosening Behaviour of Cemented Hip Prostheses Using Measurements of Migration and Inducible Displacement," J. Biomech., **35**(2), pp. 257–265.

[43] Britton, J. R., Walsh, L. A., and Prendergast, P. J., 2004, "Mechanical Simulation of Muscle Loading on the Proximal Femur: Analysis of Cemented Femoral Component Migration With and Without Muscle Loading," Clin. Biomech. (Bristol, Avon), **18**(7), pp. 637–646.

[44] Goetzen, N., Lampe, F., Nassut, R., and Morlock, M. M., 2005, "Load-Shift—Numerical Evaluation of a New Design Philosophy for Uncemented Hip Prostheses," J. Biomech., **38**(3), pp. 595–604.



Downloaded from http://risk.asmedigitalcollection.asme.org/biomechanical/article-pdf/128/4/579/5614399/579_1.pdf by guest on 02 November 2024

[45] Hung, J. P., Chen, J. H., Chiang, H. L., and Wu, J. S. S., 2004, "Computer Simulation on Fatigue Behavior of Cemented Hip Prostheses: A Physiological Model," Comput. Methods Programs Biomed., **76**(2), pp. 103–113.
[46] Nogler, M., Polikeit, A., Wimmer, C., Brückner, A., Ferguson, S. J., and Krismer, M., 2004, "Primary Stability of a ROBODOC® Implanted Anatomical Stem Versus Manual Implantation," Clin. Biomech. (Bristol, Avon), **19**(2), pp. 123–129.
[47] El'Sheikh, H. F., MacDonald, B. J., and Hashmi, M. S. J., 2003, "Finite Element Simulation of the Hip Joint During Stumbling: A Comparison Between Static and Dynamic Loading," J. Mater. Process. Technol., **143–144**, pp. 249–255.
[48] Bitsakos, C., Kerner, J., Fisher, I., and Amis, A. A., 2005, "The Effect of Muscle Loading on the Simulation of Bone Remodelling in the Proximal Femur," J. Biomech., **38**(1), pp. 133–139.

Downloaded from http://risk.asmedigitalcollection.asme.org/biomechanical/article-pdf/128/4/579/5614399/579_1.pdf by guest on 02 November 2024